UC Irvine
UC Irvine Previously Published Works

Title

Actin and microtubules drive differential aspects of planar cell polarity in multiciliated cells

Permalink

https://escholarship.org/uc/item/91w434tx

Journal

Journal of Cell Biology, 195(1)

ISSN

0021-9525

Authors

Werner, Michael E
Hwang, Peter
Huisman, Fawn
et al.

Publication Date

2011-10-03

DOI

10.1083/jcb.201106110

Peer reviewed

Actin and microtubules drive differential aspects of planar cell polarity in multiciliated cells

Michael E. Werner,[1] Peter Hwang,[1] Fawn Huisman,[2] Peter Taborek,[2] Clare C. Yu,[2] and Brian J. Mitchell[1]

[1]Department of Cell and Molecular Biology, Feinberg School of Medicine, Northwestern University, Chicago, IL 60611
[2]Department of Physics and Astronomy, University of California, Irvine, Irvine, CA 92697

Planar cell polarization represents the ability of cells to orient within the plane of a tissue orthogonal to the apical basal axis. The proper polarized function of multiciliated cells requires the coordination of cilia spacing and cilia polarity as well as the timing of cilia beating during metachronal synchrony. The planar cell polarity pathway and hydrodynamic forces have been shown to instruct cilia polarity. In this paper, we show how intracellular effectors interpret polarity to organize cellular morphology in accordance with asymmetric cellular function. We observe that both cellular actin and microtubule networks undergo drastic reorganization, providing differential roles during the polarized organization of cilia. Using computational angular correlation analysis of cilia orientation, we report a graded cellular organization downstream of cell polarity cues. Actin dynamics are required for proper cilia spacing, global coordination of cilia polarity, and coordination of metachronic cilia beating, whereas cytoplasmic microtubule dynamics are required for local coordination of polarity between neighboring cilia.

Introduction

Ciliated epithelia are found throughout nature, performing locomotor functions in a variety of aquatic organisms and providing directed fluid flow in a variety of developmental and physiological contexts. The loss of directed fluid flow in humans can result in hydrocephaly, situs inversus, infertility, and respiratory dysfunction (Zariwala et al., 2007). The epithelium of *Xenopus laevis* embryos is covered with multiciliated cells, which generate a robust flow oriented from anterior to posterior. This system has proven useful for dissecting the role that planar cell polarity (PCP) signaling and hydrodynamic forces play in orienting motile cilia (Mitchell et al., 2007, 2009; Park et al., 2008).

Individual multiciliated cells have dozens of cilia that beat in a directed manner termed rotational polarity (Wallingford, 2010). In *Xenopus* embryos, cilia rotational polarity is established during a discrete developmental window (stages 23–29). First, non–cell-autonomous PCP signaling cues instruct the orientation of ciliated cells, as reflected by a bias in the orientation of cilia beating (Park et al., 2008; Mitchell et al., 2009). This bias initiates a weak flow that establishes a positive feedback loop in which cilia respond to the prevailing hydrodynamic forces by refining their orientation until they are precisely aligned (Mitchell et al., 2007). In the ciliated epithelium of the mouse ependyma, this response to flow requires the PCP signaling molecule Van Gogh–like 2 and presumably acts through downstream mechanisms in common with the PCP pathway (Guirao et al., 2010).

Cytoskeletal rearrangements have been well characterized to be involved in generating cell polarity (Eaton, 1997; Fanto and McNeill, 2004; Vladar et al., 2009). Asymmetric accumulation of Frizzled in *Drosophila melanogaster* wing cells is driven by differential trafficking along microtubules, indicating that polarized microtubules are an integral component of early steps in cell polarity (Shimada et al., 2006; Harumoto et al., 2010). Additionally, RhoA-driven modulation of actin is downstream of PCP signaling in a variety of cell polarity events (Fanto et al., 2000; Strutt, 2001; Marlow et al., 2002). In multiciliated cells, Disheveled (Dvl) and active RhoA accumulate at the base of cilia and are required to coordinate cilia orientation (Park et al., 2008; Mitchell et al., 2009; Hirota et al., 2010). Detailed EM analysis has identified interactions between basal bodies and both actin and microtubules at the apical surface of multiciliated

The Rockefeller University Press $30.00
J. Cell Biol. Vol. 195 No. 1 19–26
www.jcb.org/cgi/doi/10.1083/jcb.201106110

JCB 19

THE JOURNAL OF CELL BIOLOGY

cells (Gordon, 1982; Lemullois et al., 1988; Sandoz et al., 1988; Chailley et al., 1989a,b). Additionally, actin and actin-interacting proteins have been implicated in basal body apical migration and docking as well as ciliogenesis (Boisvieux-Ulrich et al., 1990; Pan et al., 2007; Bershteyn et al., 2010; Kim et al., 2010; Ravanelli and Klingensmith, 2011). Here, we focus on the cellular events occurring after ciliogenesis to determine whether cytoskeletal interactions are actively involved in the polarized organization of cilia within a cell.

Results and discussion

Two distinct pools of actin form at the apical surface of multiciliated cells

Cilia nucleate from a ninefold symmetric microtubule-based structure termed the basal body, which can be reliably marked with fluorescently tagged centrin. Projecting asymmetrically off of the basal body is the basal foot, which projects in the direction of cilia beating, and the striated rootlet, which projects in the opposite direction (Steinman, 1968; Park et al., 2008). Fluorescently tagged CLAMP has been previously proposed to mark the striated rootlet because of the fact that CLAMP localization projects away from the basal body toward the nucleus in the opposite direction of cilia beating. We first analyzed the localization of actin at the base of cilia in relation to both centrin and CLAMP and observed two distinct but interconnected pools of actin at the apical surface of ciliated cells (Fig. 1, A and B). As previously reported, a meshworklike actin cap forms at the apical membrane in the same plane as basal bodies such that the ciliary axoneme emerges from the cell through holes in this meshwork (Fig. 1 A; Pan et al., 2007). Additionally, we observed a second organized pool of actin that localizes subapically, ∼0.5 µm below the cell surface (Fig. 1 B). In polarized late cells (stage 29), this second pool of actin consists of short filaments that align to connect neighboring cilia (Fig. 1 C). These actin filaments link the basal body of one cilium and the distal tip of the striated rootlet of the posterior neighboring cilium along the axis of cilia orientation (Fig. 1 E and Video 1). Early cells (stage 23) that have not established rotational polarity still have an organized apical actin meshwork; however, the subapical pool of actin is largely absent and disorganized (Fig. 1 D). Thus, this second pool connects basal bodies and rootlets to create a highly organized matrix reflecting the polarization state of the cell (Fig. 1 F). This suggests that distinct pools of actin are differentially regulated and may play distinct roles in ciliated cells.

Subapical actin is essential for the establishment of global but not local coordination of cilia polarity

The stability of actin filaments varies considerably depending on cellular function, allowing for differential targeting of distinct pools of actin with drugs that affect stability (Seagull and Heath, 1980; Gottlieb et al., 1993). We performed a dose-response analysis of the actin-depolymerizing drug cytochalasin D (Cyto D) and identified a dose (10 µM) that specifically targeted the subapical pool of actin. In Cyto D–treated embryos, we observed that the apical actin meshwork appears largely
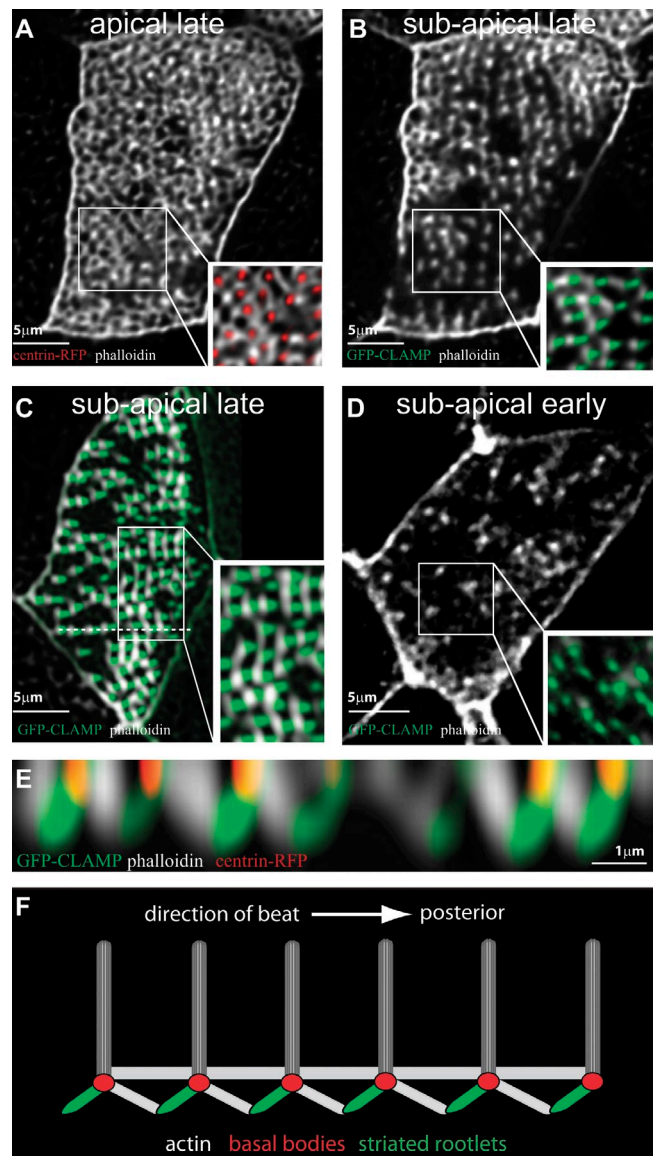

Figure 1. **Two pools of cortical actin are observable in multiciliated cells.** (A and B) Apical actin (A) forms a meshworklike network in the same plane as basal bodies, and a second pool of actin (B) localizes slightly subapically. (C and E) A late cell depicting the highly organized subapical pool of actin. The dotted line in C indicates the cross section shown in E. (D) Subapical actin in a multiciliated cell from an early embryo. (F) A diagram of subapical actin interactions with striated rootlets and basal bodies. Posterior is to the right in all panels.

intact (Fig. 2 A′). In contrast, the subapical pool of actin, bridging neighboring cilia, fails to organize in a polarized manner and is almost completely absent (Fig. 2 A″).

To determine whether this subapical pool of actin is involved in orienting cilia, we treated embryos with Cyto D during the developmental window in which cilia orientation is established (stages 23–29) and determined flow velocity, beat frequency, and cilia orientation. Cyto D treatment reduces flow velocity but does not affect either gross cilia morphology or ciliary beat frequency (Fig. 2, A, D, and E). Consistent with a reduction in flow velocity, Cyto D treatment completely blocks the establishment of coordinated cilia polarity, as reflected by a high circular SD (CSD) of 73 and a short mean vector length (vector length = 1/variance;
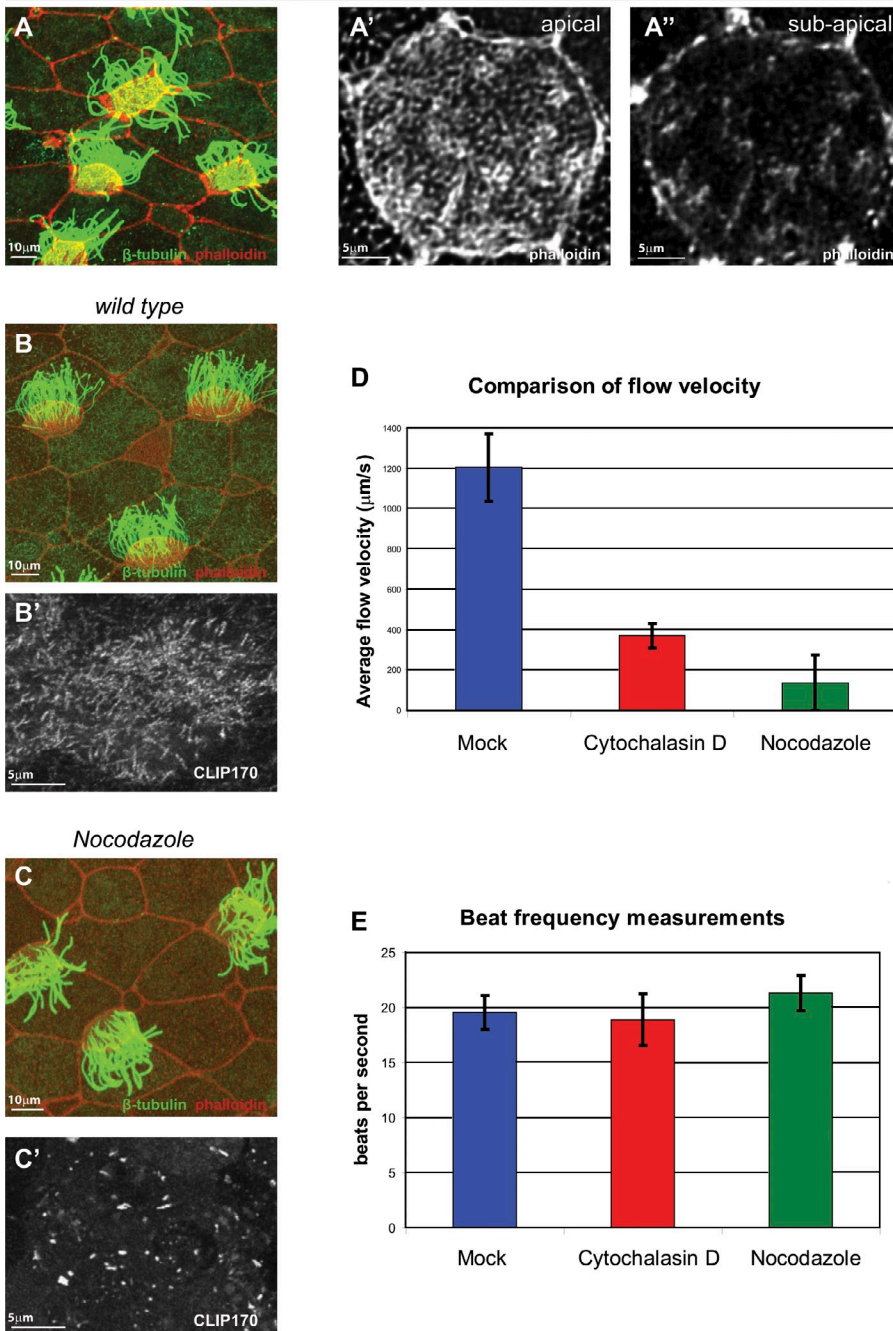
Figure 2. **Cyto D and Noc treatment affects the generation of robust fluid flow but does not affect cilia structure or beat frequency.** (A–C) Cyto D (A)–, mock (B)-, or Noc (C)-treated embryos stained with β-tubulin and phalloidin. Apical (A′) and subapical (A″) staining of actin with phalloidin of an embryo treated with 10 µM Cyto D. (B′ and C′) Images of maximum projection time-lapse videos acquired every 2 s over a 30-s time period of CLIP170-expressing embryos from control (B′) or Noc-treated cells (C′). (D) Quantification of flow velocity for embryos treated between stages 23 and 29 with mock, Cyto D, or Noc ($n = 50$, 10 flow lines from five embryos for each condition). (E) Quantification of the mean beat frequency of embryos treated between stages 23 and 29 with mock, Cyto D, or Noc ($n = 75$, five cilia from three individual cells on five different embryos for each condition). All error bars represent the SD of the mean.

Fig. 3, C and E). This CSD is significantly higher than polarized wild-type late cells (CSD = 20, P < 0.001) but is similar to unpolarized wild-type early cells (CSD = 79).

In addition to the loss of cilia polarity, we observed that cells treated with Cyto D have defective basal body spacing. Instead of distributing uniformly along the cell surface, basal bodies form clusters or long filament-like structures separated by large areas devoid of basal bodies (Fig. 3 C). We quantified this defect by scoring the distance of each individual basal body relative to its nearest neighbor (Fig. 3 F). We calculated the mean basal body nearest neighbor distribution for wild-type cells to be 0.97 µm, which is significantly decreased to 0.77 µm (P < 0.001) when subapical actin polymerization is perturbed.

Importantly, Cyto D–treated cells maintain their initial polarized bias, indicating that overall cell polarity is not lost but rather that there is a disruption in downstream cellular organization (arrow direction in Fig. 3 C). In an effort to quantify this cellular organization, we developed software that calculates angular correlation of cilia polarity as a function of distance between each basal body pair in the cell. The comparison of nearest neighbor angular correlations with farthest neighbor angular correlations allows us to quantify cellular organization and to distinguish between local coordination and global cell-wide coordination. Interestingly, whereas cell-wide coordination is completely lost, Cyto D–treated embryos maintain local coordination within individual basal body clusters, as indicated by a high nearest
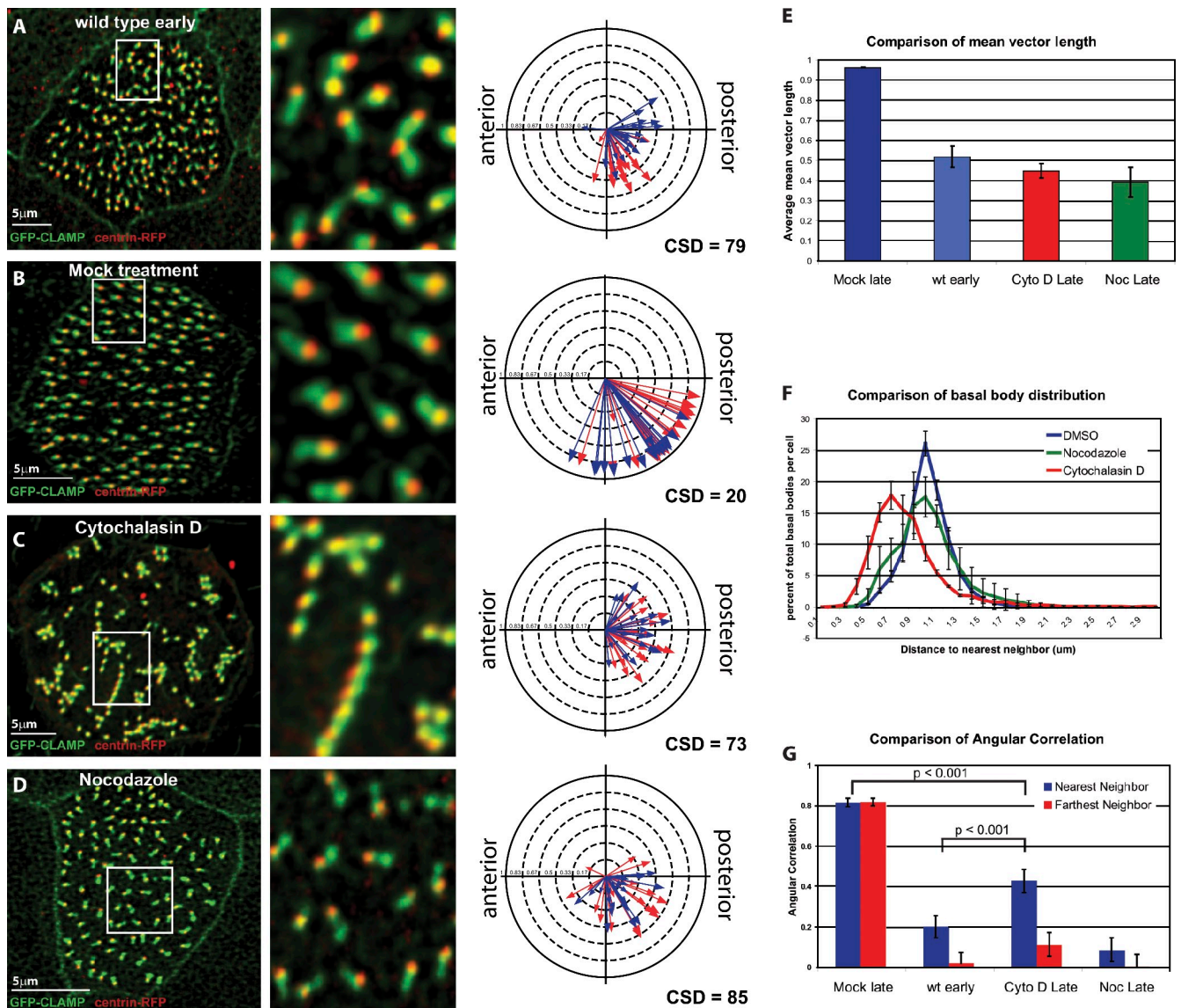
Figure 3. **Perturbation of either actin or microtubule dynamics inhibits establishment of cilia polarity.** (A–D, left) Representative images from each experimental condition. (right) Circular diagrams of mean cilia orientation (direction of arrow) as well as the variation around that mean (vector length = 1/variance) such that a short arrow represents a cell with high variance, and a long arrow represents a cell with low variance (arrow colors represent data from different embryos). (A) An untreated wild-type embryo at stage 23. (B–D) Embryos treated from stage 23–29 with 0.1% DMSO (B), 10 µM Cyto D (C), or 1 µM Noc (D). (E) Comparison of the average mean vector length (n > 60, >20 cells from at least three embryos). wt, wild type. (F) Quantification of basal body distribution by measuring the distance of individual basal bodies relative to their nearest neighbors (n > 6,000, 100–150 basal bodies from >20 cells in three embryos). (G) Angular correlation analysis for both nearest and farthest neighbor basal body pairs (n > 2,000, 100–150 basal body pairs from five cells in three embryos for each condition). All error bars represent the SD of the mean.

neighbor correlation (Fig. 3 G). This is in stark contrast to early wild-type cells that have a low level of local coordination (Fig. 3 G). This result suggests that cells with perturbed actin dynamics are still able to locally coordinate cilia orientation (high nearest neighbor angular correlation) but fail to integrate polarity information over the entire cell (high CSD and low farthest neighbor angular correlation).

Microtubule dynamics are essential for the establishment of local coordination of cilia polarity

EM studies have described elaborate interactions between basal bodies and cytoplasmic microtubules, specifically at the basal foot (Gordon, 1982; Lemullois et al., 1988; Sandoz et al., 1988; Chailley et al., 1989a). However, the function of these interactions and the consequence of interfering with them remain unknown. Because loss of actin dynamics cannot fully explain the generation of refined rotational polarity in multiciliated cells, we expanded our analysis to include microtubules. To test whether microtubule dynamics are actively involved in establishing rotational polarity, we treated embryos with various concentrations of the microtubule-depolymerizing drug nocodazole (Noc). We determined that treatment with 1 µM Noc between stages 23 and 29 did not affect either gross ciliary morphology (Fig. 2, B and C) or beat frequency (Fig. 2 E). However, using the plus-end microtubule-tracking protein CLIP170, we determined that this
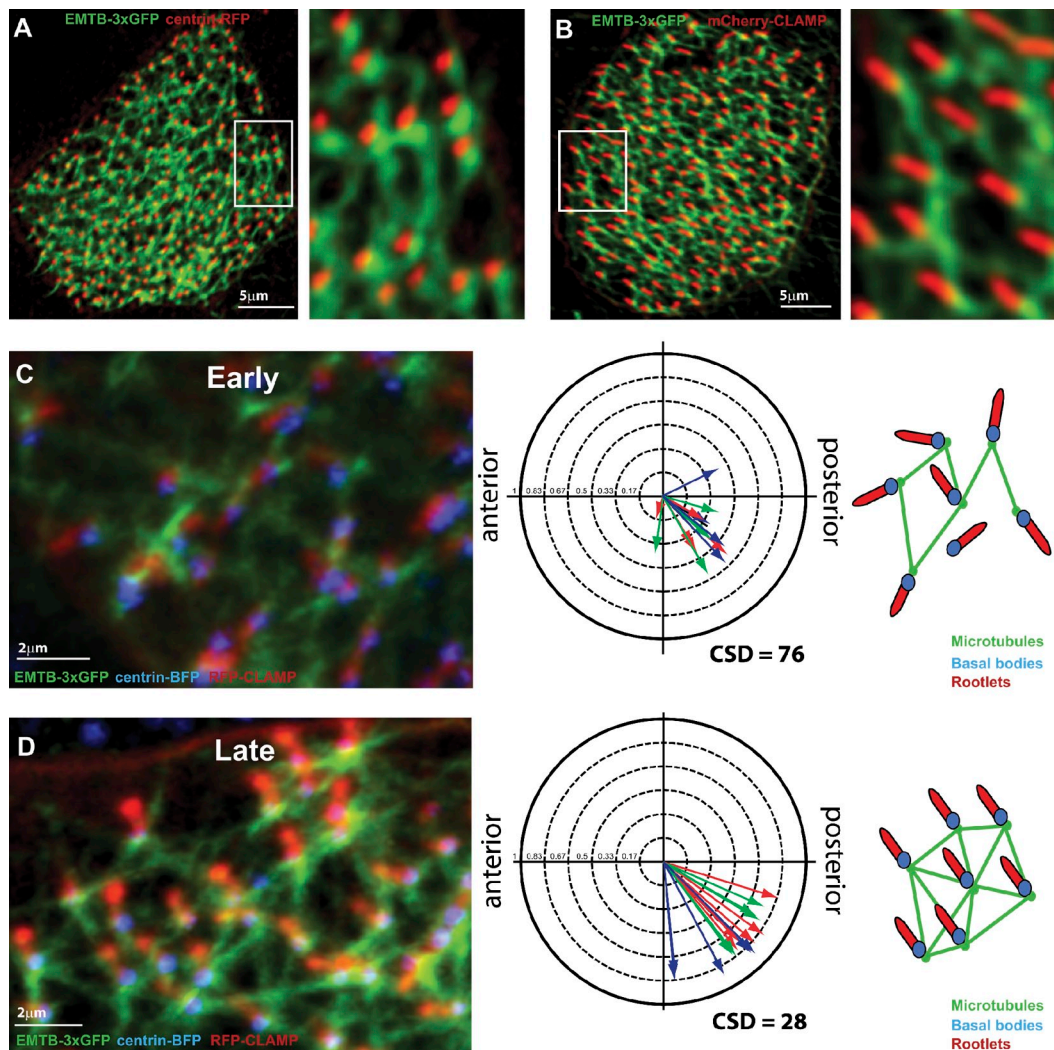
Figure 4. **Cytoplasmic microtubules form an organized network in multiciliated cells that becomes polarized during cilia refinement.** (A) A late embryo injected with the microtubule marker EMTB-3XGFP and centrin-RFP. (B) A late embryo with EMTB-3XGFP and mCherry-CLAMP. (A and B) The boxed areas are enlarged on the right. (C and D) Triple labeling with centrin–tag BFP, RFP-CLAMP, and EMTB-3XGFP in early (C) and late (D) embryos, with circular graphs of the mean position of microtubule foci relative to the nearest basal body (n > 15, five cells from three embryos) and a diagram of microtubule basal body interactions.

concentration of Noc was sufficient to inhibit cytoplasmic microtubule dynamics (Fig. 2, B' and C'; Perez et al., 1999).

Furthermore, Noc-treated embryos fail to establish robust flow but maintain a weak directed flow, similar to wild-type early embryos (Fig. 2 D). Most notably, these embryos also fail to establish rotational polarity (CSD of 85, P < 0.001; Fig. 3, D and E). In contrast to Cyto D, Noc treatment does not affect basal body distribution on the cell surface (mean distance = 0.96 µm; Fig. 3 F) but instead prevents even local coordination of cilia orientation, as indicated by a low nearest neighbor angular correlation (Fig. 3 G). Collectively, these data suggest that both cytoplasmic actin and microtubules contribute differentially to the establishment of rotational polarity. Specifically, actin is required for proper basal body spacing and global cellular organization, whereas microtubules are required for local cellular organization.

Basal bodies are equivalent to centrioles, which serve as the primary microtubule-organizing center of the cell. To determine how ciliated cells organize cytoplasmic microtubules in the presence of multiple microtubule-organizing centers, we visualized microtubules with a triple GFP–tagged version of the ensconsin microtubule-binding domain (EMTB; Bulinski et al., 2001). EMTB-3XGFP localizes to a highly organized microtubule network that forms within the plane of basal bodies in multiciliated cells (Fig. 4). Microtubules converge in bright foci in close proximity to individual basal bodies (Fig. 4, A and C–D) at the proximal end of the striated rootlet (Fig. 4, B–D). This is consistent with EM data showing microtubules enriched at the basal foot, a basal body appendage that projects 180° opposite to the striated rootlet (Sandoz et al., 1988; Park et al., 2008). In late polarized cells, microtubules consistently converge at the posterior ventral side of the nearest basal body aligned with the direction of cilia beating (Fig. 4 D, CSD = 28). In early cells, microtubules still converge in close proximity to basal bodies, but the position relative to the anterior–posterior axis is randomized (Fig. 4 C, CSD = 76). The CSD values are similar to those obtained using centrin/CLAMP (Fig. 3, A and B), indicating that
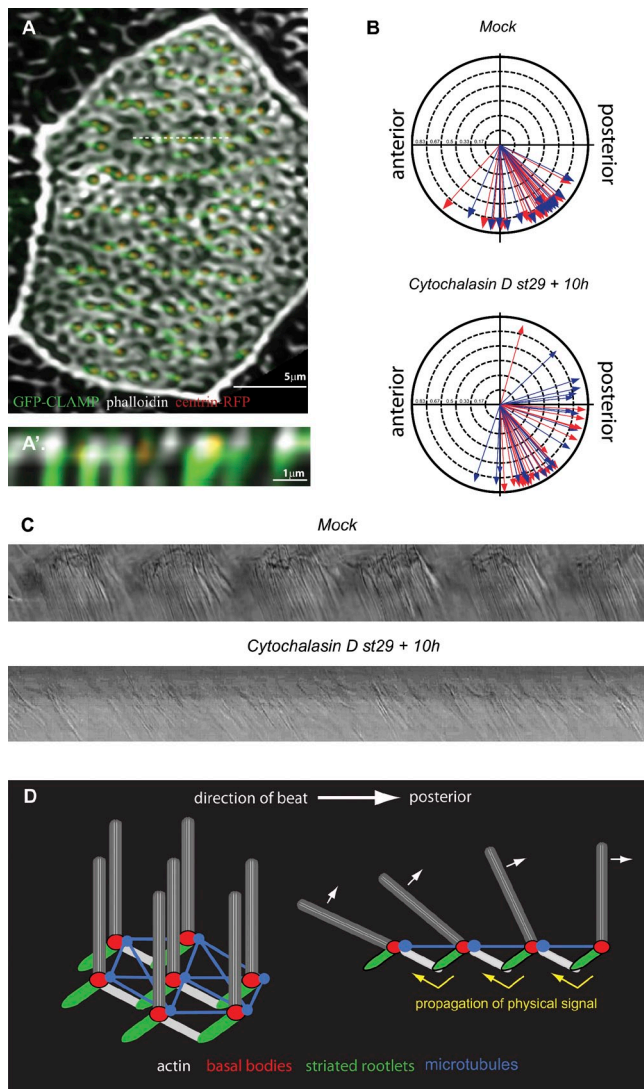
Figure 5. **Loss of subapical actin results in a loss of metachronal cilia beating.** (A) A cell from a polarized embryo treated with Cyto D with centrin-RFP and GFP-CLAMP and stained with phalloidin. The dotted line indicates the cross section in A′. (B) Circular diagrams showing mean cilia orientation from polarized embryos treated at stage 29 with either 0.1% DMSO (top) or 10 µM Cyto D (bottom) for 12 h before fixation. (C) Kymographs at cilia tips from videos of cilia beating from 0.1% DMSO (top; Video 2) and 10 µM Cyto D–treated embryos (bottom; Video 3). (D) A diagram of the high degree of polarized cytoskeletal organization in ciliated cells and the proposed model for the propagation of a physical signal involved in metachronal synchrony.

microtubule organization reflects the polarity state of the cell, which is consistent with their role in coordinating cilia polarity.

Actin bridges are required for intracellular propagation of the metachronal wave

To generate robust flow, cilia beating must be coordinated not only in direction but also in timing. Cilia at the front edge of the cell initiate the effective stroke first and are subsequently followed by more posterior cilia in a process called metachronal synchrony. The physical connection of neighboring cilia via short actin filaments linking their basal bodies to the posterior neighboring striated rootlet along the anterior–posterior axis of the cell

led us to hypothesize that these links serve as a physical lever that facilitates propagation of the metachronal wave (Fig. 5 D). To test this possibility, we treated polarized stage 29 embryos with 10 µM Cyto D, which specifically perturbs the actin bridges (Fig. 5 A) but does not perturb the already established cilia orientation (Fig. 5 B), indicating that the subapical actin pool is not involved in maintaining cilia polarity. To test whether these bridges were involved in propagating the metachronal wave, we captured high-speed videos of mature ciliated cells either mock treated or treated with Cyto D (Videos 2 and 3). Metachrony can be observed in kymographs taken above multiciliated cells that capture the passing of the effective stroke from multiple cilia as well as a pause during the recovery stroke, resulting in a discrete pattern of lines and pauses (Fig. 5 C). Significantly, in mock-treated embryos, ciliated cells maintained a highly coordinated beat pattern (Fig. 5 C and Video 2). In contrast, Cyto D–treated embryos lost coordination of cilia beating (Fig. 5 C and Video 3), indicating a loss of the metachronal wave. Because polarity and beat frequency are unperturbed in these embryos, we propose that this defect is caused by a loss in the physical connection linking the basal body of one cilium to the rootlet of its posterior neighbor.

The high degree of polar, spatial, and temporal coordination required for multiciliated cells to generate robust directed flow offers a unique view into the complexity of cell polarity. We are able to use this complexity to separate out the roles that actin and microtubules have in translating polarity cues into cellular organization. We show that both actin and microtubules form elaborate networks at the apical surface of multiciliated cells linking neighboring cilia via their basal bodies and rootlets (Fig. 5 D). Organization of these networks reflects the polarization state of the cell, and, most notably, perturbation of either of these networks leads to defects in cilia polarity. Interestingly, in the absence of cytoplasmic cytoskeletal dynamics, cilia are still capable of beating with normal beat frequencies but are unable to translate the generated hydrodynamic forces into rotational polarity. Importantly, these cells maintain their polarized bias, indicating that these defects are downstream of PCP signaling. Consistent with this, disruption of PCP cell–cell signaling leads to a loss of cell polarity but not cilia organization, whereas disruption of the PCP effector Dvl leads to a loss in both cell polarity and cilia organization (Mitchell et al., 2009).

Our data indicate that in multiciliated cells, there is an intricate interplay between actin and microtubules that is required to coordinate cell polarity. Microtubules link individual basal bodies to their neighbors via connections at their basal foot (opposite the striated rootlet) and promote local coordination of cilia orientation. In contrast, subapical actin links basal bodies to the striated rootlets of their nearest neighbor along the axis of cilia beating. These connections appear to serve multiple functions. Cells without subapical actin maintain a significant level of cellular organization, but that organization is no longer informed by global polarity cues.

The mouse ependyma has a distinct component of cell polarity termed translational polarity, in which the cilia are asymmetrically enriched on one side of the cell. This relies on signaling through a primary cilium and occurs in a myosin II–dependent manner (Hirota et al., 2010; Mirzadeh et al., 2010).

In contrast, *Xenopus* multiciliated cells, similar to the mammalian respiratory tract, lack translational polarity and have cilia that are spaced evenly over the apical surface of the cell. Our data suggest that this spacing requires interactions between neighboring cilia via subapical actin filaments. Surprisingly, interactions between neighboring basal bodies via cytoplasmic microtubules appear dispensable for proper spacing.

Finally, subapical actin connections contribute to the synchronization of cilia beating. This synchrony has been shown to require both mechanosensory regulation and a conformational switch in the outer dynein arms (Rompolas et al., 2010). Considerable modeling efforts have suggested that this coordination is derived from hydrodynamic coupling (Gueron et al., 1997; Guirao and Joanny, 2007; Yang et al., 2008). We hypothesize that, in addition to purely hydrodynamic forces, physical links in the form of actin bridges propagate a mechanical signal that is required for the generation of a metachronal wave.

Materials and methods

Plasmids and mRNA
The basal body marker centrin (UniGene accession no. Xl.50473) was cloned into pCS2+ and was C-terminally fused with either GFP or RFP, and the rootlet marker CLAMP (UniGene accession no. Xl.26316) was cloned into pCS2+ and was N-terminally fused with GFP, RFP, or mCherry (Park et al., 2008). Cilia were labeled with GFP-Xl.16654, which was amplified by PCR from *Xenopus* cDNA using the primers 5′-GCCTCGA-GATGTTCAAAAACACCTTCCA-3′ and 5′-GCTCTAGATTGCTTGGCTTT-ATTCTGTA-3′ and cloned into pCS2-GFPN3 with XhoI and XbaI. To make pCS2–tag BFPN1, TagBFP (Evogen, Inc.) was amplified by PCR, cut with BamHI and BglII, and cloned into the BamHI site of pCS2+. BFP-centrin was generated by amplifying centrin from pCS2–centrin-RFP and by cloning into pCS2–tag BFPN1. Plasmids were linearized with NotI, and mRNA was generated by in vitro transcription using SP6 RNA polymerase as previously described (Sive et al., 2000). The pCS2–EMTB-3XGFP was a gift from W. Bement (University of Wisconsin, Madison, WI), and the pCS2-CLIP170 was a gift from L. Davidson (University of Pittsburgh, Pittsburgh, PA).

mRNA injection and drug treatments
Xenopus embryos were obtained by in vitro fertilization using standard protocols (Sive et al., 2000) approved by the Northwestern University Institutional Animal Care and Use Committee. Purified mRNA was injected into two– or four–cell stage embryos into all blastomeres. Embryos were incubated at 16–25°C in 0.1× Marc's Modified Ringer's with gentamicin until they reached the desired developmental stage. Noc (Sigma-Aldrich) and Cyto D (Sigma-Aldrich) were used at final concentrations of 1 µM and 10 µM, respectively. Optimal concentrations were determined from dilution series using the lowest drug concentration that showed significant effects on actin or microtubule organization. Final dilutions were obtained by diluting 1,000× stocks in 0.1× Marc's Modified Ringer's with gentamicin. When embryos were treated at stage 23, they were incubated in the presence of the drug overnight at 16°C until they reached stage 29. When embryos were treated at stage 29, they were incubated in the presence of the drug for 12 h at 16°C.

Immunofluorescence
Embryos were fixed in 3% PFA in 80 mM K$^+$ Pipes, pH 6.8, with 2 mM MgCl$_2$ and 5 mM EDTA for 2 h. Embryos were blocked for 1 h with 5% normal donkey serum in PBS 0.1% Triton X-100. The following primary antibodies were used according to the manufacturer's recommended dilutions: mouse anti–β-tubulin (7–10; Developmental Studies Hybridoma Bank), mouse antiacetylated α-tubulin (T7451; Sigma-Aldrich), and Cy-2–, Cy-3–, or Cy-5–conjugated secondary antibodies (Jackson Immuno-Research Laboratories, Inc.). To visualize actin, we used phalloidin 568 or 647 (Invitrogen). Embryos were mounted between two coverslips using Fluoro-Gel (Electron Microscopy Sciences).

Microscopy
All immunofluorescence, as well as measurements of cilia beat frequency, was performed on a laser-scanning confocal microscope (A1R; Nikon)

using a 60× oil Plan-Apo objective with a 1.4 NA. Beating of fluorescently labeled cilia was imaged using resonance-scanning confocal microscopy at 240 frames per second over a 5-s time period. Images were acquired using Elements software (Nikon). To determine flow velocity, we used a digital camera (165FC and DFC295; Leica) to visualize the displacement of 10 µm FluoSpheres polystyrene microspheres (yellow-green fluorescent 505/515; Invitrogen) along the skin of live embryos. Flow videos were acquired using Application Suite software (Leica), and flow velocities were scored using Elements software. High-speed videos of cilia beating were captured at 6,688 frames per second on a Phantom camera (7.2; Vision Research) mounted on a microscope (BX51; Olympus) with a 100× objective. All microscopy was performed at room temperature.

Image processing and quantifications
Images were deconvolved using AutoQuant Blind deconvolution in Elements software. Cilia orientation was scored as previously described (Mitchell et al., 2007, 2009; Park et al., 2008). In brief, individual rootlet orientation was scored manually by measuring the angle of orientation of the rootlets relative to the anterior–posterior axis of the embryo using Elements software. Excel (Microsoft) and Oriana 2.0 software were used for graphical representation of the datasets and to calculate mean vector length and CSD. Cilia beat frequency was scored using kymographs to capture the effective stroke of an individual cilium over a 5-s time period. Basal body spacing was calculated by determining the absolute position of individual basal bodies using Elements software and by calculating the distance of each basal body to its nearest neighbor using a custom macro in Excel.

Angular correlation analysis
Angular correlation analysis was performed using a custom program. After determining absolute coordinates for basal bodies and distal tips of associated rootlets, unit vectors (length = 1) were constructed that pointed from the basal body to the rootlet tip of each cilia in a ciliated cell. Let A = (A_x, A_y) and B = (B_x, B_y) denote two such vectors. The angular correlation is the dot product A • B = $A_x B_x + A_y B_y = \cos(\theta)$, in which θ is the angle between the vectors if their tails (basal bodies) were at the same point. The angular correlation (dot product) varies between −1 and +1. The distance between the basal bodies was computed and gives the separation.

Online supplemental material
Video 1 shows complex interactions between actin, basal bodies, and rootlets. Video 2 shows metachronal synchrony of cilia beating. Video 3 shows loss of metachronal synchrony after treatment with Cyto D. Online supplemental material is available at http://www.jcb.org/cgi/content/full/jcb.201106110/DC1.

References

Bershteyn, M., S.X. Atwood, W.M. Woo, M. Li, and A.E. Oro. 2010. MIM and cortactin antagonism regulates ciliogenesis and hedgehog signaling. *Dev. Cell*. 19:270–283. http://dx.doi.org/10.1016/j.devcel.2010.07.009

Boisvieux-Ulrich, E., M.C. Lainé, and D. Sandoz. 1990. Cytochalasin D inhibits basal body migration and ciliary elongation in quail oviduct epithelium. *Cell Tissue Res.* 259:443–454. http://dx.doi.org/10.1007/BF01740770

Bulinski, J.C., D.J. Odde, B.J. Howell, T.D. Salmon, and C.M. Waterman-Storer. 2001. Rapid dynamics of the microtubule binding of ensconsin in vivo. *J. Cell Sci.* 114:3885–3897.

Chailley, B., G. Nicolas, and M.C. Lainé. 1989a. Organization of actin microfilaments in the apical border of oviduct ciliated cells. *Biol. Cell*. 67:81–90.

Chailley, B., T. Frappier, F. Regnouf, and M.C. Laine. 1989b. Immunological detection of spectrin during differentiation and in mature ciliated cells from quail oviduct. *J. Cell Sci.* 93:683–690.

Eaton, S. 1997. Planar polarization of *Drosophila* and vertebrate epithelia. *Curr. Opin. Cell Biol.* 9:860–866. http://dx.doi.org/10.1016/S0955-0674(97)80089-0

Fanto, M., and H. McNeill. 2004. Planar polarity from flies to vertebrates. *J. Cell Sci.* 117:527–533. http://dx.doi.org/10.1242/jcs.00973

Fanto, M., U. Weber, D.I. Strutt, and M. Mlodzik. 2000. Nuclear signaling by Rac and Rho GTPases is required in the establishment of epithelial planar polarity in the *Drosophila* eye. *Curr. Biol.* 10:979–988. http://dx.doi.org/10.1016/S0960-9822(00)00645-X

Gordon, R.E. 1982. Three-dimensional organization of microtubules and microfilaments of the basal body apparatus of ciliated respiratory epithelium. *Cell Motil.* 2:385–391. http://dx.doi.org/10.1002/cm.970020407

Gottlieb, T.A., I.E. Ivanov, M. Adesnik, and D.D. Sabatini. 1993. Actin microfilaments play a critical role in endocytosis at the apical but not the basolateral surface of polarized epithelial cells. *J. Cell Biol.* 120:695–710. http://dx.doi.org/10.1083/jcb.120.3.695

Gueron, S., K. Levit-Gurevich, N. Liron, and J.J. Blum. 1997. Cilia internal mechanism and metachronal coordination as the result of hydrodynamical coupling. *Proc. Natl. Acad. Sci. USA.* 94:6001–6006. http://dx.doi.org/10.1073/pnas.94.12.6001

Guirao, B., and J.F. Joanny. 2007. Spontaneous creation of macroscopic flow and metachronal waves in an array of cilia. *Biophys. J.* 92:1900–1917. http://dx.doi.org/10.1529/biophysj.106.084897

Guirao, B., A. Meunier, S. Mortaud, A. Aguilar, J.M. Corsi, L. Strehl, Y. Hirota, A. Desoeuvre, C. Boutin, Y.G. Han, et al. 2010. Coupling between hydrodynamic forces and planar cell polarity orients mammalian motile cilia. *Nat. Cell Biol.* 12:341–350. http://dx.doi.org/10.1038/ncb2040

Harumoto, T., M. Ito, Y. Shimada, T.J. Kobayashi, H.R. Ueda, B. Lu, and T. Uemura. 2010. Atypical cadherins Dachsous and Fat control dynamics of noncentrosomal microtubules in planar cell polarity. *Dev. Cell.* 19:389–401. http://dx.doi.org/10.1016/j.devcel.2010.08.004

Hirota, Y., A. Meunier, S. Huang, T. Shimozawa, O. Yamada, Y.S. Kida, M. Inoue, T. Ito, H. Kato, M. Sakaguchi, et al. 2010. Planar polarity of multiciliated ependymal cells involves the anterior migration of basal bodies regulated by non-muscle myosin II. *Development.* 137:3037–3046. http://dx.doi.org/10.1242/dev.050120

Kim, J., J.E. Lee, S. Heynen-Genel, E. Suyama, K. Ono, K. Lee, T. Ideker, P. Aza-Blanc, and J.G. Gleeson. 2010. Functional genomic screen for modulators of ciliogenesis and cilium length. *Nature.* 464:1048–1051. http://dx.doi.org/10.1038/nature08895

Lemullois, M., E. Boisvieux-Ulrich, M.C. Laine, B. Chailley, and D. Sandoz. 1988. Development and functions of the cytoskeleton during ciliogenesis in metazoa. *Biol. Cell.* 63:195–208. http://dx.doi.org/10.1016/0248-4900(88)90058-5

Marlow, F., J. Topczewski, D. Sepich, and L. Solnica-Krezel. 2002. Zebrafish Rho kinase 2 acts downstream of Wnt11 to mediate cell polarity and effective convergence and extension movements. *Curr. Biol.* 12:876–884. http://dx.doi.org/10.1016/S0960-9822(02)00864-3

Mirzadeh, Z., Y.G. Han, M. Soriano-Navarro, J.M. García-Verdugo, and A. Alvarez-Buylla. 2010. Cilia organize ependymal planar polarity. *J. Neurosci.* 30:2600–2610. http://dx.doi.org/10.1523/JNEUROSCI.3744-09.2010

Mitchell, B., R. Jacobs, J. Li, S. Chien, and C. Kintner. 2007. A positive feedback mechanism governs the polarity and motion of motile cilia. *Nature.* 447:97–101. http://dx.doi.org/10.1038/nature05771

Mitchell, B., J.L. Stubbs, F. Huisman, P. Taborek, C. Yu, and C. Kintner. 2009. The PCP pathway instructs the planar orientation of ciliated cells in the *Xenopus* larval skin. *Curr. Biol.* 19:924–929. http://dx.doi.org/10.1016/j.cub.2009.04.018

Pan, J., Y. You, T. Huang, and S.L. Brody. 2007. RhoA-mediated apical actin enrichment is required for ciliogenesis and promoted by Foxj1. *J. Cell Sci.* 120:1868–1876. http://dx.doi.org/10.1242/jcs.005306

Park, T.J., B.J. Mitchell, P.B. Abitua, C. Kintner, and J.B. Wallingford. 2008. Dishevelled controls apical docking and planar polarization of basal bodies in ciliated epithelial cells. *Nat. Genet.* 40:871–879. http://dx.doi.org/10.1038/ng.104

Perez, F., G.S. Diamantopoulos, R. Stalder, and T.E. Kreis. 1999. CLIP-170 highlights growing microtubule ends in vivo. *Cell.* 96:517–527. http://dx.doi.org/10.1016/S0092-8674(00)80656-X

Ravanelli, A.M., and J. Klingensmith. 2011. The actin nucleator Cordon-bleu is required for development of motile cilia in zebrafish. *Dev. Biol.* 350:101–111. http://dx.doi.org/10.1016/j.ydbio.2010.11.023

Rompolas, P., R.S. Patel-King, and S.M. King. 2010. An outer arm Dynein conformational switch is required for metachronal synchrony of motile cilia in planaria. *Mol. Biol. Cell.* 21:3669–3679. http://dx.doi.org/10.1091/mbc.E10-04-0373

Sandoz, D., B. Chailley, E. Boisvieux-Ulrich, M. Lemullois, M.C. Laine, and G. Bautista-Harris. 1988. Organization and functions of cytoskeleton in metazoan ciliated cells. *Biol. Cell.* 63:183–193. http://dx.doi.org/10.1016/0248-4900(88)90057-3

Seagull, R.W., and I.B. Heath. 1980. The differential effects of cytochalasin B on microfilaments populations and cytoplasmic streaming. *Protoplasma.* 103:231–240. http://dx.doi.org/10.1007/BF01276269

Shimada, Y., S. Yonemura, H. Ohkura, D. Strutt, and T. Uemura. 2006. Polarized transport of Frizzled along the planar microtubule arrays in *Drosophila* wing epithelium. *Dev. Cell.* 10:209–222. http://dx.doi.org/10.1016/j.devcel.2005.11.016

Sive, H., R.M. Grainger, and R.M. Harland. 2000. Early Development of Xenopus laevis: a laboratory manual. Cold Spring Harbor Press, Plainview, NY. 338 pp.

Steinman, R.M. 1968. An electron microscopic study of ciliogenesis in developing epidermis and trachea in the embryo of *Xenopus laevis. Am. J. Anat.* 122:19–55. http://dx.doi.org/10.1002/aja.1001220103

Strutt, D. 2001. Planar polarity: getting ready to ROCK. *Curr. Biol.* 11:R506–R509. http://dx.doi.org/10.1016/S0960-9822(01)00305-0

Vladar, E.K., D. Antic, and J.D. Axelrod. 2009. Planar cell polarity signaling: the developing cell's compass. *Cold Spring Harb. Perspect. Biol.* 1:a002964. http://dx.doi.org/10.1101/cshperspect.a002964

Wallingford, J.B. 2010. Planar cell polarity signaling, cilia and polarized ciliary beating. *Curr. Opin. Cell Biol.* 22:597–604. http://dx.doi.org/10.1016/j.ceb.2010.07.011

Yang, X., R.H. Dillon, and L.J. Fauci. 2008. An integrative computational model of multiciliary beating. *Bull. Math. Biol.* 70:1192–1215. http://dx.doi.org/10.1007/s11538-008-9296-3

Zariwala, M.A., M.R. Knowles, and H. Omran. 2007. Genetic defects in ciliary structure and function. *Annu. Rev. Physiol.* 69:423–450. http://dx.doi.org/10.1146/annurev.physiol.69.040705.141301